

# Unsteady MHD Boundary Layer Flow of an Incompressible Micropolar Fluid over a Stretching Sheet

K. Govardhan<sup>1†</sup> and N. Kishan<sup>2</sup>

<sup>1</sup>*Department of Engineering Mathematics, GITAM University, Viilge Rudraram, Medak Dist, Hyderabad-502329, A.P. INDIA.*

<sup>2</sup>*Department of mathematics, Osmania University, Hyderabad 500007, A.P. India*

†Corresponding Author Email: [govardhan\\_kmtm@yahoo.co.in](mailto:govardhan_kmtm@yahoo.co.in)

(Received April 22, 2010; accepted June 22, 2011)

## ABSTRACT

Aim of the paper is to investigate the MHD effects on the unsteady boundary layer flow of an incompressible micropolar fluid over a stretching sheet when the sheet is stretched in its own plane. The stretching velocity is assumed to vary linearly with the distance along the sheet. Two equal and opposite forces are impulsively applied along  $x$  – axis so that the sheet is stretched, keeping the origin fixed in a micropolar fluid. The governing non-linear equations and their associated boundary conditions are first cast into dimensionless form by a local non-similarity transformation. The resulting equations are solved numerically using the Adams- Predictor Corrector method for the whole transient from the initial state to final steady- state flow. Numerical results are obtained and a representative set is diapaced graphically to illustrate the influence of the various physical parameters on the velocity profiles, microrotation profiles as well as the Skin friction coefficient for various values of the material parameter  $K$ . It is found that there is a smooth transition from the small- time solution to the large- time solution. Results for the local skin friction coefficient are presented in table as well as in graph.

**Keywords:** Unsteady flow, Micro polar fluid, Stretching surface, Skin friction, MHD.

## NOMENCLATURE

$B_0$	applied magnetic field	$u, v$	velocity components
$j$	micro-inertia	$x, y$	cartesian co-ordinates
$k$	vortex viscosity	$\rho$	density of the fluid
$K$	matériel parameter	$\sigma$	electrical conductivity
$M$	magnetic field parameter	$\gamma$	Spin gradient
$n$	constant	$\mu$	dynamic viscosity
$N$	micro rotation		

## 1. INTRODUCTION

The fluid dynamics over a stretching surface is important in extrusion process. The production of sheeting material arises in a number of industrial manufacturing process and includes both metal and polymer sheets. Examples are numerous and they include the cooling of an infinite metallic plate in a cooling bath, the boundary layer along material handling conveyers, the aerodynamic extrusion of plastic sheets, the boundary layer along a liquid film in condensation process, paper production, glass blowing, metal spinning, and drawing plastic films, to name just a few. The quality of the final product depends on the rate of heat transfer at the stretching surface. A comprehensive review of micropolar fluids mechanically has been presented by [Ariman et al.](#)

(1973). Since the pioneering study by [Crane \(1970\)](#) who presented an analytical solution for the steady two – dimensional stretching of a surface in a quiescent fluid, many authors have considered various aspects of this problem and obtained similar solutions. Some mathematical results were presented by many authors, and a good number of references can be found in the papers by [Magyari and Keller \(1999,2000\)](#). [Sriramulu et al. \(2001\)](#) studied steady flow and heat transfer of a viscous incompressible fluid through porous medium over a stretching sheet.

On the other hand, it is well known that the theory of micropolar fluids has generated a lot of interest and many flow problems have been studied. The theory of micropolar fluids was originally developed by [Eringen](#)

(1964,1966) and has now been applied in the investigation of various fluids. The theory takes into account the microscopic effects arising from the local structure and micro-motions of the fluid elements and provides the basis for a mathematical model for non-newtonian fluids which can be used to analysis the behaviour of exotic lubricants, polymers, liquid crystals, animal bloods and colloidal or suspension solutions, etc. Since introduced by Eringen many researchers have considered various problems in micropolar fluids. Nazar *et al.* (2004) studied the stagnation point flow of a non-Newtonian micropolar fluids with zero vertical velocity at the surface or heat generation. Rajeshwari and Nath (1992) studied unsteady flow over a stretching surface in a rotating fluid, Noor (1992) investigated Heat transfer from a stretching sheet.

Guram and Smith (1980) investigated the stagnation flows of micropolar fluids with strong and weak interactions. They obtained numerical results using a fourth order Runge – Kutta method. Gorla (1983) obtained numerical results by a Runge – Kutta method for the micropolar boundary layer flow at a stagnation point on a moving wall. Heat transfer over a stretching surface with variable surface heat flux in micropolar fluids and MHD stagnation point flow towards a stretching vertical sheet in a micropolar fluid is studied by Ishak *et al.* (2008). Recently Nazar *et al.* (2008) studied the unsteady boundary layer flow of an incompressible micropolar fluid over a stretching sheet. They solved numerically using Keller-box method. Viscous dissipation effects were consider on mhd nonlinear flow and heat transfer past a stretching porous surface embeded in a porous medium under a transverse magnetic field is studied Anjalidevi and ganga(2010). Sharma and singh(2009) is investigated the effect of variable thermal conductivity and heat source/sink on flow of a viscous incompressible electrically conducting fluid in the presence of uniform transverse magnetic fluid and variable free stream near a stagnation point on a non conducting stretching sheet.

The purpose of the present paper is to study the magneto hydrodynamic effects on the unsteady boundary layer flow of an incompressible micropolar fluid over a stretching sheet when the sheet is stretched in its own plane. A numerical solution is obtained for the governing momentum using the Adams predictor-corrector method.

**2. MATHEMATICAL ANALYSIS**

Consider the flow of an incompressible micropolar fluid in the region  $y > 0$  driven by a plane surface located at  $y = 0$  with a fixed end at  $x = 0$ . It is assumed that the surface is stretched in the  $x$ -direction such that the  $x$ -component of the velocity varies linearly along it, i.e.  $u_w(x) = cx$ , where  $C$  is an arbitrary constant and  $c > 0$ . The simplified two - dimensional equations governing the flow are the equations of the continuity, momentum equations under the influence of externally imposed transverse magnetic field in the boundary layer steady laminar and incompressible micropolar fluids are;

$$\frac{\partial u}{\partial x} + \frac{\partial v}{\partial y} = 0 \tag{1}$$

$$\frac{\partial u}{\partial t} + u \frac{\partial u}{\partial x} + v \frac{\partial u}{\partial y} = \left(\frac{\mu+k}{\rho}\right) \frac{\partial^2 u}{\partial y^2} + \frac{k}{\rho} \frac{\partial N}{\partial y} - \frac{\sigma B_0^2}{\rho} u \tag{2}$$

$$\rho j \left( \frac{\partial N}{\partial t} + u \frac{\partial N}{\partial x} + v \frac{\partial N}{\partial y} \right) = \gamma \frac{\partial^2 N}{\partial y^2} - k \left( 2N + \frac{\partial u}{\partial y} \right) \tag{3}$$

Subject to the initial and boundary conditions

$$\begin{aligned} t \leq 0 : u = v = N = 0, \text{ for any } x, y, \\ t > 0 : v = 0, u = u_w(x) = cx, N = -n \frac{\partial u}{\partial y}, \text{ at } y = 0, \\ u \rightarrow 0, \text{ as } y \rightarrow \infty, N \rightarrow 0 \end{aligned} \tag{4}$$

Where  $u$  and  $v$  are the velocity components along the  $x$ - and  $y$ - axes, respectively,  $t$  is time,  $N$  is the microrotation or angular velocity whose direction of rotation is in the  $xy$ - plane,  $\mu$  is dynamic viscosity,  $\rho$  is density,  $j$  is microinertia per unit mass,  $\gamma$  is spin gradient viscosity and  $k$  is vortex viscosity. Further,  $n$  is a constant and  $0 \leq n \leq 1$ . The case  $n = 0$ , which indicates  $N=0$  at the wall represents concentrated particle flows in which the microelements close to the wall surface are unable to rotate. This case is also known as the strong concentration of microelements. The case  $n = 1/2$  indicates the vanishing of anti - symmetric part of the stress tensor and denotes weak concentration of microelements. The case  $n = 1$  is used for the modeling of turbulent boundary layer flows. We shall consider here both cases of  $n = 0$  and  $n = 1/2$ .

Introducing the new variables as

$$\begin{aligned} \psi = (cv)^{1/2} \xi^{1/2} x f(\xi, \eta), N = (c/v)^{1/2} \xi^{-1/2} cxg(\xi, \eta), \\ \eta = (c/v)^{1/2} \xi^{-1/2} y, \xi = 1 - e^{-\tau}, \tau = ct, \end{aligned} \tag{5}$$

Where  $\psi$  is the stream function defined in the usual way as

$$u = \frac{\partial \psi}{\partial y} \text{ and } v = -\frac{\partial \psi}{\partial x}, \text{ and identically satisfy Eq. (1).}$$

Substituting variables (5) in to Eqs. (2) and (3) gives

$$\begin{aligned} (1+K)f''' + (1-\xi)\frac{\eta}{2}f'' + \xi(f'f'' - f'^2 - Mf') \\ + Kg' = \xi(1-\xi)\frac{\partial f'}{\partial \xi} \end{aligned} \tag{6}$$

$$\begin{aligned} \left(1 + \frac{K}{2}\right)g'' + (1-\xi)\left(\frac{1}{2}g + \frac{\eta}{2}g'\right) + \xi(fg' - f'g) \\ - K\xi(2g + f'') = \xi(1-\xi)\frac{\partial g}{\partial \xi} \end{aligned} \tag{7}$$

Where  $K = \frac{k}{\mu}$  is the material parameter. Here  $\gamma$  and  $j$  are assumed to be given by  $\gamma = \left(\mu + \frac{k}{2}\right)j = \mu\left(1 + \frac{K}{2}\right)j$  and  $j = \frac{\nu}{c}$ , respectively.

The boundary conditions Eq. (4) becomes

$$f(\xi, 0) = 0, f'(\xi, 0) = 1, g(\xi, 0) = -nf''(\xi, 0),$$

$$f'(\xi, \infty) = 0, g(\xi, \infty) = 0. \tag{8}$$

The physical quantity of interest in this problem is the skin friction coefficient  $C_f$ , which is defined as

$$C_f = \frac{\tau_w}{\rho u_w^2 / 2}, \tag{9}$$

Where  $\tau_w$  is the skin friction, given by

$$\tau_w = \left[ (\mu + k) \frac{\partial u}{\partial y} + kN \right]_{y=0}. \tag{10}$$

Using variables (5) in Eqs. (9) and (10), we obtain

$$C_f Re_x^{1/2} = \xi^{-1/2} [1 + (1-n)K] f''(\xi, 0). \tag{11}$$

Further, we can obtain some particular cases of this problem.

### A. Early Unsteady Flow

For early unsteady flow  $0 < \tau \ll 1$ , we have  $\xi \approx 0$ , so Eqs. (6) and (7) reduce in the leading order approximation to

$$(1+K)f''' + \frac{\eta}{2}f'' + Kg' = 0, \tag{12}$$

$$\left(1 + \frac{K}{2}\right)g'' + \frac{\eta}{2}g' + \frac{1}{2}g = 0, \tag{13}$$

and the boundary conditions (8) become

$$f(0) = 0, f'(0) = 1, g(0) = -nf''(0),$$

$$f'(\infty) = 0, g(\infty) = 0. \tag{14}$$

### B. Final steady- state Flow

For this case,  $\xi = 1$  and Eqs. (6) and (7) take the following forms:

$$(1+K)f''' + f f'' - f'^2 - Mf' + Kg' = 0 \tag{15}$$

$$\left(1 + \frac{K}{2}\right)g'' + f g' - f' g - K(2g + f'') = 0 \tag{16}$$

Subject to the boundary conditions (14).

## 3. METHOD OF SOLUTION

To solve the Eqs. (6) and (7), we have convert into a system of five first order equations, we have at

$$\xi + \Delta\xi, (y_1 \rightarrow f, y_4 \rightarrow g), y_1' = y_2, y_2' = y_3$$

$$y_3' = \left[ \begin{array}{l} \xi(1-\xi)y_2(\xi + \Delta\xi) - y_2(\xi) - (1-\xi)\frac{\eta}{2}y_3 + \\ \xi(y_1y_3 - y_2^2 - M^*y_2) - ky_5 \end{array} \right],$$

$$/(1+k)$$

$$y_4' = y_5 \text{ and}$$

$$y_5' = \left[ \begin{array}{l} \xi(1-\xi)\frac{y_4(\xi + \Delta\xi) - y_4(\xi)}{\Delta\xi} - (1-\xi)\left(\frac{1}{2}y_4 + \frac{\eta}{2}y_5\right) \\ -\xi(y_1y_5 - y_2y_4) \end{array} \right] / \left(1 + \frac{k}{2}\right)$$

Early unsteady flow is obtained by solving these equations with  $\xi = 0$ . For  $\xi > 0$ , the above equations reflect a fully implicit scheme with respect to  $\xi$ . In both cases, assuming  $y_3(\xi, 0) = \alpha$  and  $y_5(\xi, 0) = \beta$ , the above system is solved up to  $\eta_{\max} (\approx \infty)$ .

To solve  $\alpha$  and  $\beta$  by Newton-Raphson method. We need  $\frac{\partial y_2}{\partial \alpha}, \frac{\partial y_4}{\partial \alpha}, \frac{\partial y_2}{\partial \beta}$  and  $\frac{\partial y_4}{\partial \beta}$  at  $\eta = \eta_{\max}$ , these quantities are obtained by solutions

$$y_1' = y_2, y_2' = y_3,$$

$$y_3' = \left[ \begin{array}{l} \xi(1-\xi)\frac{\partial y_2(\xi + \Delta\xi)}{\Delta\xi} - (1-\xi)\frac{\eta}{2}y_3 \\ +\xi(y_1y_3 + Y_1y_3 - 2y_2y_2 - M^*y_2) - ky_5 \end{array} \right] / (1+k) \quad y_4' = y_5$$

and

$$y_5' = \left[ \begin{array}{l} \xi(1-\xi)\frac{y_4(\xi + \Delta\xi)}{\Delta\xi} - (1-\xi)\left(\frac{1}{2}y_4 + \frac{\eta}{2}y_5\right) + \\ \xi(y_1y_5 + Y_1y_5 - y_2y_4 - Y_2y_4) \end{array} \right] / \left(1 + \frac{k}{2}\right)$$

Once with

$$y_1(0) = y_2(0) = 0, y_3(0) = 0, y_4(0) = -n,$$

$$y_5(0) = 0$$

and another time with

$$y_1(0) = y_2(0) = 0, y_3(0) = 0, y_4(1) = 0, y_5(0) = 1.$$

This procedure converging in about three iterations giving correct values of  $\alpha$  and  $\beta$ . The system of Ordinary differential equation is solved by Adams predictor-corrector methods of fourth order. Accuracy is ensured by solving with different  $\Delta\xi, \eta_{\max}, \Delta\eta$ .

## 4. DISCUSSION OF THE RESULTS

The transformed Eqs. (6) and (7) satisfying the boundary conditions (8) were solved numerically using the Adams predictor-corrector method for several values of the material parameter  $K$ . Numerical results for Skin friction coefficients, the velocity distribution and microrotation distribution are shown graphically.

To validate our method we have compared the Skin friction coefficients  $C_f Re_x^{1/2}$  values with Rosilinda Nazar (2008) is shown in Table1, there is very good agreement between the results when we solved fully unsteady boundary layer equations and final steady state equations. Though computations have been carried out for various values of the  $n$  and the material parameter  $K$  are presented.

**Table 1** Values of the skin friction coefficient  $C_f Re_x^{1/2}$  for various values of  $K$  and  $n$  when  $\xi = 1$ .

$K/n$	0	1/2
0	-1.0043	-1.0043
1	-1.3952	-1.24005
2	-1.6635	-1.4532
4	-2.0092	-1.8105

The velocity distribution of initial flow ( $\xi = 0$ ) and unsteady flow ( $0 < \xi \leq 1$ ) for various values of  $K$  with  $n = 0$  and  $n = 1/2$  is shown graphically in Figs. 1 and 2 respectively. From both the figures it is observed that the velocity boundary layer thickness increases with the increasing values of  $K$ , for both the cases  $n = 0$  and  $n = 1/2$ . The Figs. 3 and 4 represent for final steady state flow ( $\xi = 1$ ) for the cases  $n = 0$  and  $n = 1/2$ , respectively.

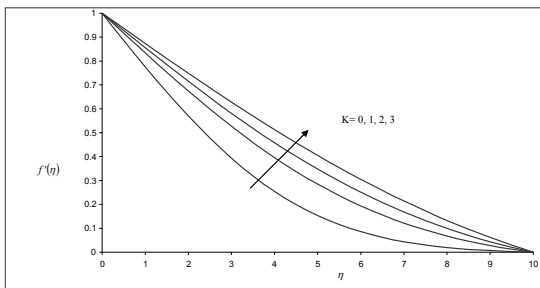


**Fig. 1.** Velocity distribution of initial flow ( $\xi = 0$ ) and early unsteady flow ( $0 < \xi \ll 1$ ) for various  $K$  with  $n = 0$

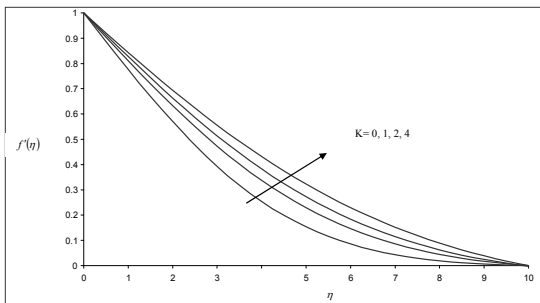


**Fig. 2.** Velocity distribution of initial flow ( $\xi = 0$ ) and early unsteady flow ( $0 < \xi \ll 1$ ) for various  $K$  with  $n = 1/2$

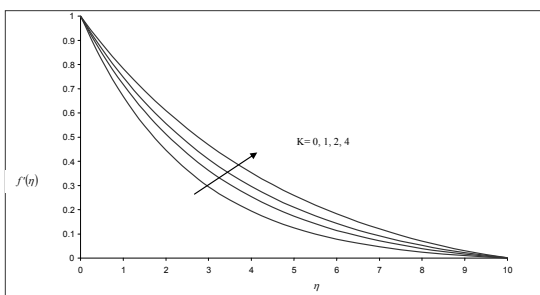


**Fig. 3.** Velocity distribution of final steady-state flow ( $\xi = 1$ ) for various  $K$  with  $n = 0$

It is observed from the figures that the velocity increases with the increase of  $K$ . The velocity

distribution of fully developed unsteady flow ( $0 < \xi < 1$ ) and final steady state flow ( $\xi = 1$ ) is represented in the Figs. 5 and 6 for the cases  $n = 0$  and  $n = 1/2$ , respectively.

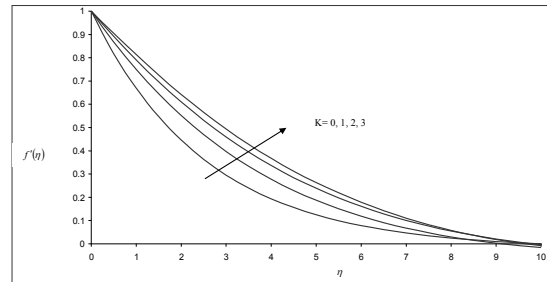


**Fig. 4.** Velocity distribution of final steady-state flow ( $\xi = 1$ ) for various  $K$  with  $n = 1/2$

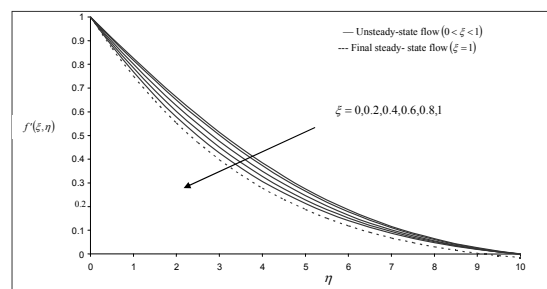


**Fig. 5.** Velocity distribution of fully developed unsteady flow for  $K=1$  when  $n = 0$

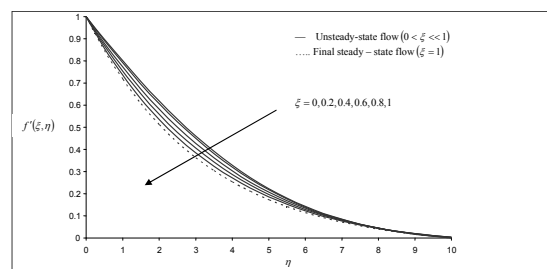


**Fig. 6.** Velocity distribution of fully developed unsteady flow for  $K=1$  when  $n = 1/2$

These figures show that the velocity profiles corresponding to increasing of  $\xi$  ( $0 < \xi \leq 1$ ) approach the final steady profile corresponding to  $\xi = 1$ . It has seen that there is a smooth transition from small time solution ( $\xi \approx 0$ ) to large time solution ( $\xi = 1$ ).

The effect of magnetic parameter  $M$  on velocity distribution  $f'(\eta)$  is shown in Fig. 7. The magnetic field parameter  $m$ , effect is shown in Fig. 7 for the velocity distribution  $f'(\eta)$  of final steady flow ( $\xi = 1$ ) with  $K = 1$  and  $n = 0$ . The velocity distribution of final steady state flow ( $\xi = 1$ ) for various  $M$  values with  $K = 1$ ,  $n = 0$  is shown in Fig. 7. It is obvious that existence of Magnetic field  $M$  decelerates the velocity profiles. Figures 8-13 represents microrotation distribution for various values of  $K$ ,  $n$  for steady state and unsteady state flow. The microrotation distribution of final steady state flow ( $\xi = 1$ ) is increases with the

increase of the material parameter  $K$  is observed from Fig. 8 when  $n = 0$ .

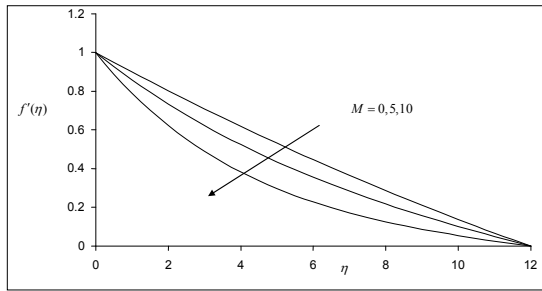


**Fig. 7.** Velocity distribution of final steady-state flow ( $\xi = 1$ ) for various  $M$  with  $n = 0$  and  $K = 1$

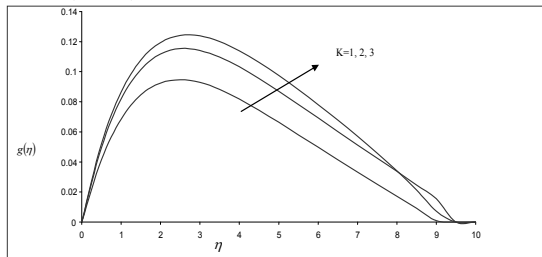


**Fig. 8.** Micro rotation distribution of final steady-state flow ( $\xi = 1$ ) for various  $K$  when  $n = 0$

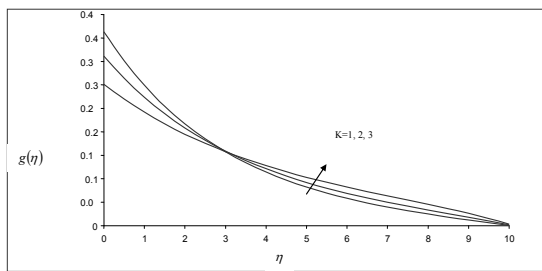


**Fig. 9.** Micro rotation distribution of final steady-state flow ( $\xi = 1$ ) for various  $K$  when  $n = 1/2$

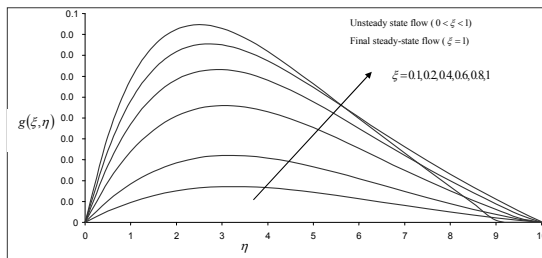


**Fig. 10.** Micro rotation distribution of fully developed unsteady flow for  $n = 0$  and  $K = 1$

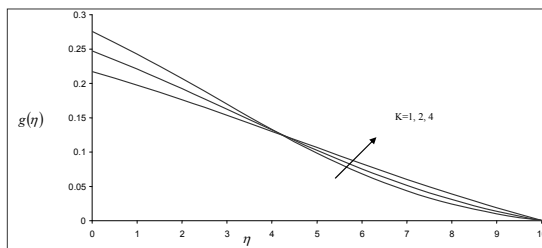
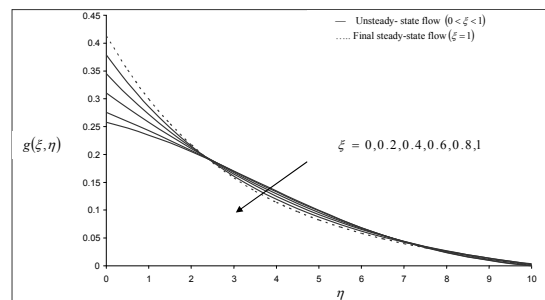


**Fig. 11.** Micro rotation distribution of early unsteady flow ( $0 < \xi \ll 1$ ) for various  $K$  with  $n = 1/2$

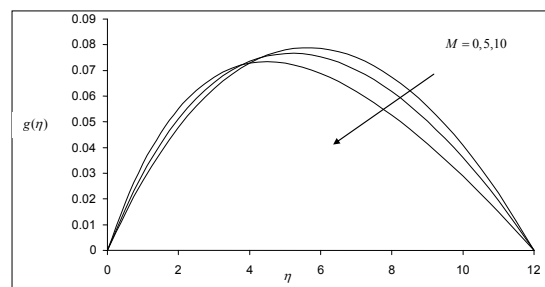
The microrotation distribution of final steady state flow ( $\xi = 1$ ) with  $n = 1/2$  is shown in Fig.9, from which the microrotation decreases as  $K$  increases in the vicinity of the plate where as it increases as one moves away from it. Fig. 10 represents the microrotation distribution of fully developed unsteady flow for  $n = 0$  and  $K = 1$  for  $0 < \xi \leq 1$ . It is noticed that the microrotation distribution as parabolic distribution and increases with the increase of  $\xi$ .

Figure 11 shows that microrotation distribution of early unsteady flow ( $0 < \xi < 1$ ) for various  $K$  values with  $n = 1/2$ . The microrotation distribution decreases as  $K$  increases near the plate but reverse phenomena is observed as one moves away from the plate. The microrotation distribution of fully developed unsteady flow when  $K = 1$  and  $n = 1/2$  and final steady state flow ( $\xi = 1$ ) is shown in Fig.12. The microrotation distribution increases near the plate while, the reverse happens far away the plate with the increase of  $\xi$  is observed.

The magnetic field effect on the microrotation distribution is plotted in Fig. 13. It can be seen from the figure that the magnetic field effect accelerates the microrotation distribution near the plate, where as it decelerates the microrotation distribution far away from the plate. The magnetic field effect is more on microrotation distribution when far away from the plate.



**Fig. 12.** Microrotation distribution of fully developed unsteady flow for  $n = 1/2$  and  $K = 1$



**Fig. 13.** Micro rotation distribution of final steady-state flow ( $\xi = 1$ ) for various  $M$  when  $K = 1$ ,  $n = 0$ .

The Skin friction coefficient  $C_f Re_x^{1/2}$  with  $\xi$  for various values of  $K$  is drawn when  $n = 0$  in Fig. 14 and  $n = 1/2$  in Fig.15. It can be seen that the values of  $C_f Re_x^{1/2}$  decreases as  $K$  increases.

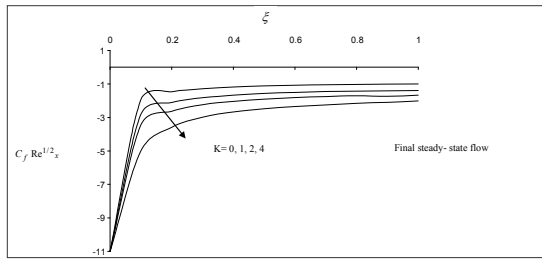


**Fig. 14.** Variation with  $\xi$  of the skin friction coefficient for various  $K$  with  $n = 0$

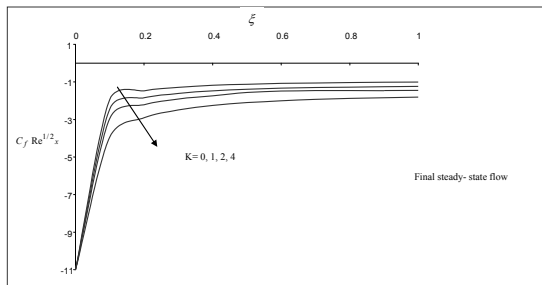


**Fig. 15.** Variation with  $\xi$  of the skin friction coefficient for various  $K$  with  $n = 1/2$

## 5. CONCLUSION

It is clear from the figures that the microrotation effects are more pronounced for  $n = 1/2$  when compared to those of  $n = 0$ . The microrotation profile for  $n = 0$  is different as compared to  $n = 1/2$  it has a parabolic distribution when  $n = 0$ , where as it has continuously decreasing when  $n = 1/2$ . The values of the Skin friction coefficients for the final steady flow are shown in Table 1. It is noticed that due to impulsive motion, the skin friction coefficients as large magnitude (absolute value) for small time ( $\tau \approx 0$  or  $\xi \approx 0$ ) after the start of the motion, and decreases monotonically and reaches the steady state value at  $\xi = 1$  ( $\tau \rightarrow \infty$ ). The magnetic field effect is to decelerate the velocity distribution  $f'(\eta)$ . The microrotation distribution of final steady flow ( $\xi = 1$ ) is to increase near the plate, where as it decreases far away from the plate with the effect of magnetic field are observed.

## ACKNOWLEDGEMENT

I thank you for referees, their valuable suggestions for making my paper more lucid

## REFERENCES

Anjalidevi, S.P and B. Ganga (2010). Dissipation effects on MHD nonlinear flow and heat transfer past a porous medium with prescribed heat flux. *Journal of Applied Fluid Mechanics* 13(5), 1-6.

Ariman, T., M.A. Turk and N.D. Sylvester (1973). Microcontinuum fluid mechanics- a review. *Int. J. Eng. Sci.* 11, 905-930.

Crane, L.J. (1970). Flow Past a stretching Plane. *Journal of Applied Mathematics and Physics (ZAMP)* 21, 645-647.

Eringen, A.C. (1964). Simple micropolar fluids. *Int. J. Engng. Sci.* 2, 205-217.

Eringen, A.C. (1966). Theory of micropolar fluids. *J. Math. Mech* 16, 1-18.

Gorla, R.S.R. (1983). Micropolar boundary layer flow at stagnation point on a moving wall. *Int. J. Engng. Sci.* 21, 25-33.

Guram, G.S. and A.C. Smith (1980). Stagnation flows of micropolar fluids with strong and weak interaction. *Comp. Maths. with Appls.* 6, 213-233.

Ishak, A., R. Nazar and I. Pop (2008). Heat transfer over a stretching surface with variable surface heat flux in micropolar fluids. *Phys. Lett. A* 372, 559-561.

Magyari, E. and B. Keller (2000). Exact Solutions for Self – Similar Boundary – Layer Flows induced by Permeable Stretching Surfaces. *European Journal of Mechanics B – fluids* 19, 109-122.

Magyari, E. and B. Keller (1999). Heat and Mass Transfer in the Boundary Layers on an Exponentially Stretching Continuous Surface. *Journal of Physics D: Applied Physics* 32, 577-586.

Nazar, R., N. Amin, D. Filip and I. Pop (2004). Stretching point flow of a Micropolar Fluid towards a stretching sheet. *Int. J. non-Linear Mech.* 39, 1227-1235.

Noor, A. (1992). Heat transfer from a stretching sheet. *Int J Heat and Mass Transfer* 4, 1128-1131.

Rajeshwari, V. and G. Nath (1992). Unsteady flow over a stretching surface in a rotating fluid. *Int. J. Eng. Sci.* 30(6), 747-756.

Roslinda, N., A. Ishak, and I. Pop (2008). Unsteady Boundary Layer Flow Over a Stretching Sheet in a Micropolar Fluid. *International Journal of Mathematical, Physical and Engineering Sciences* 2(3), 161-165.

Sharma, P.R. and G. Singh (2009). Effect of variable thermal conductivity and heat source/ sink on MHD flow near a stagnation point on linearly stretching sheet. *Journal of Applied Fluid Mechanics* 2(1, 3), 13-21.

Sriramulu, A., N. Kishan and J. Anadarao (2001). Steady flow and heat transfer of a viscous incompressible fluid flow through porous medium over a stretching sheet. *Journal of Energy, Heat and Mass Transfer* 23, 483-495.